J Mol Model (2009) 15:165–171
DOI 10.1007/s00894-008-0412-y

ORIGINAL PAPER

A disulfide linked model of the complement protein C8γ complexed with C8α indel peptide

Athanassios Stavrakoudis

Received: 6 June 2008 / Accepted: 28 July 2008 / Published online: 2 December 2008

Abstract In a recent study C8γ (complement protein) with Cys40Ala substitution and a C8α derived peptide with Cys164Ala substitution were co-crystallized and their binding mode was revealed. Computer modeling and molecular dynamics simulations were performed in order to check the hypothesis that the residues Ala164 of C8α and Ala40 of C8γ occupied the right position if cysteine residues were in their place for disulfide bonding. Substitution of these two alanine residues with cysteine along with disulfide bond creation via molecular modeling and subsequent molecular dynamics simulation of the complex corroborated the hypothesis, which was also confirmed from recent crystallographic data. Average RMSD between backbone atoms of the indel peptide during the MD trajectory in comparison with the corresponding sequence of crystal structure of the C8α/γ complex was found only 0.085 nm.

Keywords C8α/γ complex · Complement protein · Computer simulation · Membrane attack complex · Molecular dynamics

Introduction

Membrane attack complex (MAC) [1] is a cytolytically active macromolecular complex assembled on the surface of pathogenic organisms. It has five components: C5b, C6, C7, C8, and C9. Human C8 is composed by three genetically distinct subunits: α (64 kDa), β (64 kDa) and γ (22 kDa). C8α and C8γ form a C8 α-γ heterodimer which is linked through a disulfide bond and this in turn associates non-covalently with C8β [2, 3]. C8γ protein belongs to the lipocalin family and it is unrelated to any other member of the complement. Until now C8γ [4] and C8α MACPF domain [5] are the only MAC protein with known 3D structures, although the structure of the associated dimmer is not known. C8γ fold is similar to other structures of lipocalin family proteins [6], while C8α has a fold similar to cytolysins [5], and they are pore forming cholesterol-dependent proteins.

Mapping the binding sites of C8α complement protein to other C8 subunits [7, 8] has revealed a 19mer peptide to be responsible for C8γ binding. A smaller fragment of 11 residues (indel peptide) was also capable of biological activity.

Recently, the crystal structure between C8γ and an indel peptide of C8α sequence has been published [6]. In this complex, both Cys_{40} of C8γ and Cys_{164} of C8α chains respectively were substituted by Ala residues. These two cysteine residues form the disulfide bond of the heterodimer C8α-γ. The peptide L_{158}RYDSTAERLY$_{168}$ is a minimal sequence from the C8α protein that binds to the C8γ. Interestingly, it contains the Cys_{164} residue that forms a disulphide bond with Cys_{40} of C8γ, when C8α and C8γ complement protein associate into a heterodimer.

In order to check this hypothesis and further provide evidence the C8γ association with C8α derived peptide through disulfide bond, molecular modeling and computer simulation techniques were applied [9,10]. Starting from the C8γ/C8α indel peptide X-Ray structure [6], both Ala_{164} and Ala_{40} residues of C8α and C8γ chains respectively

Electronic supplementary material The online version of this article (doi:10.1007/s00894-008-0412-y) contains supplementary material, which is available to authorized users.

A. Stavrakoudis (✉)
Department of Economics, University of Ioannina,
45110 Ioannina, Greece
e-mail: astavrak@cc.uoi.gr

were replaced with cysteine residues and a disulfide bond was imposed between them. The heterodimer complex was subjected to molecular dynamics simulation in explicit water in order to extract the dynamical properties of association and to examine the stability of the proposed disulfide bonded complex. Results revealed that the heterodimeric complex is stable, under MD conditions, and support the association hypothesis.

Very recently, Slade et al. published [11] the crystal structure of the C8γ/C8α complex. These crystallographic data corroborated the association hypothesis and provided a validation framework of the current study and the proposed model.

Materials and methods

Initial complex coordinates were extracted from X-Ray structure as deposited at PDB [12], access code 2qos [6]. Residues Ala_{164} of the C8γ chain and Ala_{40} of the C8α chain were replaced with cysteine residues and a disulfide bond was imposed between them using the VMD program [13]. Protonation status of histidine side chains was estimated with the REDUCE program [14]. Topology and force field parameters for all atoms where assigned from the CHARMM27 parameter set [15]. The complex was solvated with 15505 TIP3P [16] water molecules using a rectangular box with dimensions $7.835 \times 7.971 \times 8.581$ nm^3. Na^+ and Cl^- ions were also placed into the system for charge neutralization and ionic strength mimic of 0.1 nm NaCl using the autoionize plugin of VMD (15 Na^+ and 14 Cl^- were placed). MM/MD runs were performed with NAMD (v2.6) [17]. Non-bonded van der Waals interactions were gradually turned off at a distance between 1.0 and 1.2 nm. Long range electrostatics were computed at every first step with the PME [18] method. Non-bonded forces and PME electrostatics were calculated every second step. Pair list was updated every 10 steps. Bonds to hydrogen atoms were constrained with the SHAKE algorithm [19] allowing a 2 fs time step for integration. The whole system (consisted by 49420 atoms) was initially subjected to energy minimization with 5000 steps. The temperature of the system was then gradually increased with Langevin dynamics, using the NVT ensemble, to 310 K, during a period 3000 steps, by stepwise reassignment of velocities every 500 steps. During minimization and equilibration phases, backbone atoms (N, C^{α}, C', O) of the peptide or protein chains were restrained to their initial positions with a force constant of 50 $kcalmol^{-1}Å^{-2}$. The simulation continued until 100,000 steps (0.2 ns). The force constant of positional restraints was then decreased to 5 $kcalmol^{-1}$ $Å^{-2}$ for other 100,000 steps and finally positional restraints were totally eliminated for subsequent 200,000 steps of NVT equilibration period. The simulation was continued under constant pressure with Langevin piston method [20] for 15 ns. Pressure was maintained at 1 atm and temperature was kept at 310 K. Snapshots were saved to disk at 1 ps interval for further analysis.

A second (control) simulation was also carried out starting from the same X-Ray structure, but without imposing the disulfide bond, in order to test the stability of the complex. This simulation was performed under identical conditions with the previous one and for the same time. To avoid confusion between the two simulations, the first one (covalent complex) is named S1 and the second one (non-covalent complex) is named S2.

Conformational analysis performed with VMD [13] and Carma [21]. Secondary structure assignment was analyzed with the program STRIDE [22]. Hydrogen bonds were measured with geometrical criteria: Hydrogen-Acceptor distance less than 0.25 nm and Donor-Hydrogen-Acceptor angle greater than 120°. Structural figures were prepared with PYMOL [23]. Averaged quantities form trajectory frames are followed by corresponding standard deviations in parentheses.

Results and discussion

RMSD and RMSF analysis

Structural superimposition of the complex structure before and after the disulfide bond, as well as superimposition of representative structures from S1 trajectory, is shown in Fig. 1. Visual inspection of the structures reveals the goodness of fit between the experimental and the modeled structure as well as the conformational stability of the indel peptide as modeled with disulfide bond linkage with the C8γ protein.

Root mean square fluctuation of C8γ and C8α/peptide C^{α} atoms during the MD trajectory of covalent complex (S1) was found to be relatively small, typically less than 0.1 nm (Fig. 2). This fact indicates the relative stability of the complex structure, which remained relatively close to the initial structure. C^{α} atoms of C8γ/peptide Cys_{164} and adjacent residues Thr_{163} and Glu_{165} showed RMSF values between 0.050 and 0.053 nm. Time evolution of RMSD of backbone atoms (Fig. 2c), of either C8α indel peptide or C8γ chains, after superimposition of trajectory frames over the starting structure (X-Ray) also remained stable and with values less than 0.2 nm (Fig. 2c). Both RMSF and RMSD analysis provide evidence for the relative stability of the complex and indicate the feasibility of the proposed structure, thus the disulfide linking between C8γ and indel peptide via residues Cys40 and Cys164 respectively.

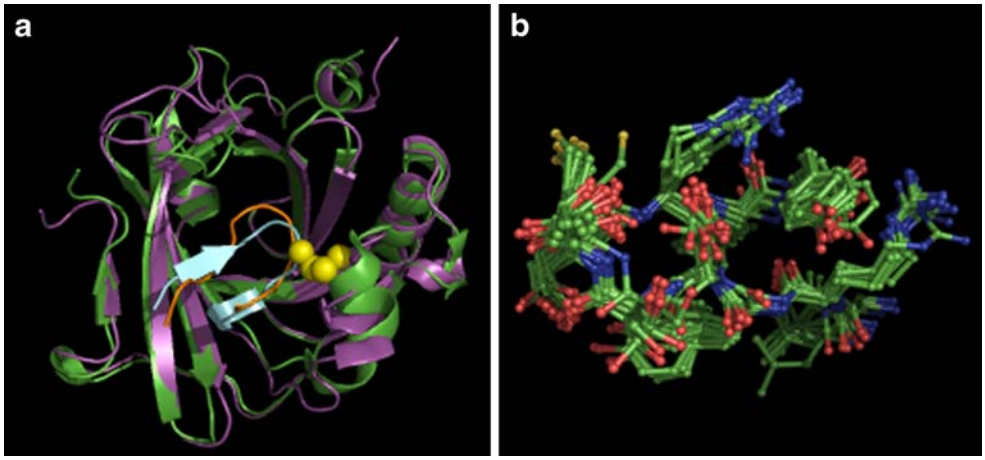

Fig. 1 **a**) Backbone atoms superimposition of the initial (X-Ray) and final (frame 15000) structures. The disulfide link (atoms C^{β}, S^{γ}) is represented with balls. Chain C (C8γ protein) is represented with green (starting structure) and purple (final structure) ribbons respectively. Chain A (C8α indel peptide) is represented with cyan (starting structure) and orange (final structure) ribbons respectively. **b**) Bundle of ten indel peptide structures, superimposed over heavy atoms. One frame every 1.5 ns were obtained. Structures were fitted with RMSD slightly less than 0.06 nm. For the interpretation of colors in this figure the reader is referred to the online version of this article

Very recently the structure of the C8γ complement protein complexed with C8α [11] has been released from Protein Data Bank. In this structure the two protein chains form a heterodimer via a disulfide bond between C8γ Cys_{40} and C8α Cys_{164}. The C8α protein chain contained the indel peptide sequence L_{158}RYDSTAERLY$_{168}$. The modeled structure of the current MD study and the crystal structure of C8α protein (concerning the fragment 158-168) showed significant similarity as revealed by RMSD analysis (Fig. 2c). The observed values between 0.08 and 0.14 nm demonstrated the successful modeling of the C8γ/C8α disulfide association.

Backbone conformation and secondary structure of the peptide

Secondary structure assignment of the initial structure of the indel peptide revealed that its conformation was in CCEEGGGCEEC state, forming two short β-strands connected by a turn [6]. Arg_{159}←Tyr_{168}, Asp_{161}←Ala_{164},

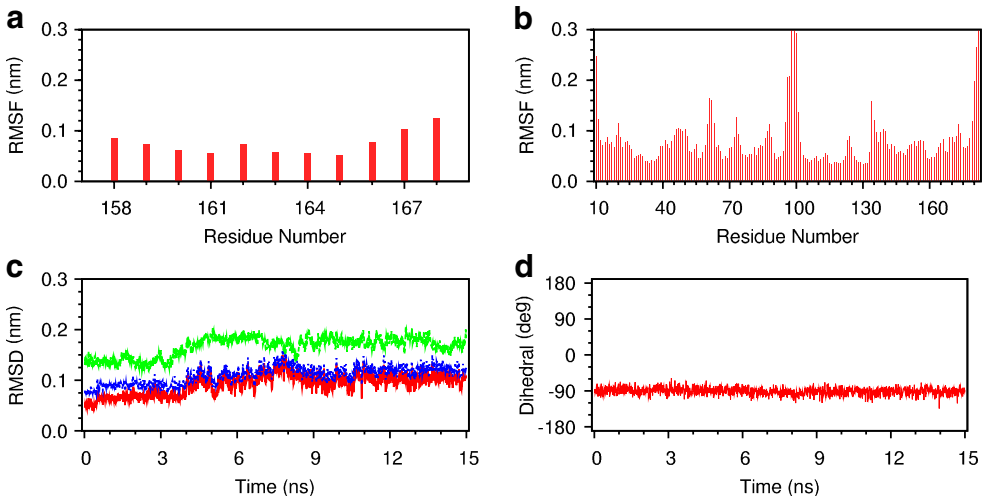

Fig. 2 Results from S1 (covalent structure) simulation. **a**) Root mean square fluctuation of the C^{α} atoms of the C8α indel peptide. **b**) Root mean square fluctuation of C^{α} atoms of the C8γ protein. **c**) Time evolution of RMSD of backbone atoms of C8α indel peptide over starting structure (red line), C8γ protein over starting structure (green line) and C8α indel peptide over the corresponding fragment of C8α protein complexed with C8γ (blue line). **d**) time evolution of the dihedral angle around the S-S bond between C8γ Cys_{40} and C8α Cys_{164}. For the interpretation of colors in this figure the reader is referred to the online version of this article

Asp_{161}←Arg_{166}, Ser_{162}←Glu_{165} and Arg_{166}←Asp_{161} main chain hydrogen bonds stabilized this secondary structure. During MD trajectory, the secondary structure of the indel peptide changed slightly to CCEETTTTEEC (41.1% of the MD trajectory), which was the dominant conformational state of the peptide (Table 1). Similar conformational states CCBTTTTTCBC (28.1%) and CCBTTTTCCBC (16.8%) were also observed for shorter periods of time. The two β-strands of the peptide (residues Tyr_{160}-Asp_{161} and Arg_{166}-Leu_{167}) remained relative stable, although turn, bend or coil conformational transitions were observed for small fragment of the trajectory. Residues close to N- or C-terminal part of the peptide were found in coil conformation. In general, backbone dihedral angles showed only minor fluctuation around averaged values without major transitions during MD trajectory (see supplement).

Two consecutive β-turns were observed in the middle part of the peptide sequence, instead of a $_{3\text{-}10}$helix found in residues Ser_{162}-Ala_{164} in the crystal structure.

Residues Ser_{162}-Thr_{163} constituted the central part of the first turn, which was found to be type IV according to STRIDE analysis. Backbone dihedral angles φ,ψ of these residues did not show significant fluctuation during MD trajectory and averaged at values [-97.4° (16.2°), -45.2° (14.8°)] and [-75.1° (14.2o), -62.2° (11.8°)] for residues Ser_{162} and Thr_{163} respectively. Main chain hydrogen bond Asp_{161}←Cys_{164} that could stabilize this turn was not observed. Anyway, distance of C^{α} atoms of residues Asp_{161} and Cys_{164} and dihedral angle (absolute value) of C^{α} atoms of residues Asp_{161}-Ser_{162}-Thr_{163}-Cys_{164} remained below 0.7 nm and 90° respectively for 99.3% of the simulating time.

Residues Thr_{163}-Cys_{164} constituted the central part of the second β-turn which was found to be type VIII according to STRIDE analysis, again without main chain hydrogen bond stabilization. Backbone dihedral angles φ,ψ of Thr_{163} and Cys_{164} averaged at values [-75.1° (14.2°), -62.2° (11.8°)] and [-95.8° (13.0°), 145.9° (32.5°)] for residues Thr_{163} and Cys_{164} respectively. The distance of C^{α} atoms of residues Ser_{162} and Glu_{165} and dihedral angle (absolute value) of C^{α} atoms of residues Ser_{162}-Thr_{163}-Cys_{164}-Glu_{165} remained below 0.7 nm and 90° respectively for 66.5% of the simulating time, indicating the reduced stability of this second β-turn.

The antiparallel β-strand conformation of the C8α indel peptide bound into the C8γ calyx was also stabilized by a Arg_{159}←Tyr_{168} and Arg_{166}←Asp_{161} main chain hydrogen bonds which were found in 75.3% and 86.9% of the simulation time respectively (Table 2). Tyr_{168}'s backbone carbonyl oxygen atom was also found in hydrogen bond state with either Arg_{159}:$N^{\eta 2}$ or Arg_{159}:N in 65.0% and 23.3% of the simulation time respectively. According to STRIDE conformational assignment of trajectory structures, strand conformation of residues Tyr_{160}-Asp_{161} and Arg_{166}-Leu_{167} was observed only in approximately half of the trajectory frames. However, backbone bone dihedral angle analysis revealed only minor differences between starting values (PDB structure) and trajectory averages (see also supplement). For example, ϕ,ψ dihedral angles of Arg_{166} were found -108.8° and 125.8° in the crystal structure. These dihedral angle were averaged at -129.7° (24.4°) and 132.9° (21.4°) respectively. The relative stability of peptide's secondary structure, with only minor perturbations observed during MD trajectory, indicates that the imposed disulfide bond did not alter significantly the backbone conformation of the indel peptide.

Disulfide bond dynamics

Dihedral angle around disulfide bond (measured by $Cys_{C8\gamma 40}$: C^{β} – $Cys_{C8\gamma 40}$: S^{γ} – $Cys_{C8\alpha 164}$: S^{γ} – $Cys_{C8\alpha 164}$: C^{β} atoms) fluctuated around -90.9° (9.2°), in agreement with the experimentally determined structure of C8α/C8γ complex where the corresponding value was found -91.3°. No conformational transition around the S-S bond was observed during the time scale of the simulation (Fig. 2d), which indicates the relative stability of the disulfide bonded

Table 1 Clusters of conformational assignment of the indel peptide during S1 trajectory calculated with STRIDE

Cluster	Conformational assignment											Percentage
	L	R	Y	D	S	T	C	E	R	L	Y	
1	C	C	E	E	T	T	T	T	E	E	C	41.1
2	C	C	B	T	T	T	T	T	C	B	C	28.1
3	C	C	B	T	T	T	T	C	C	B	C	16.8
4	C	C	B	T	T	T	T	T	T	B	C	7.5

Percentage of frames is given out of 15,000 total frames stored. Four main clusters were observed with population over 5% during the MD trajectory. The sequence of the peptide is given in the first line. STRIDE shortcuts: C for coil, E for strand, T for turn and B for bridge conformational states respectively.

Table 2 Hydrogen bonding of the indel peptide (intramolecular hydrogen bonds) or the C8γ/peptide (intermolecular hydrogen bonds)

Donor	Acceptor	% in S1
$Arg_{\alpha 159}$: N	$Tyr_{\alpha 168}$: O	23.3
$Arg_{\alpha 159}$: $N^{\eta 2}$	$Tyr_{\alpha 168}$: O	65.0
$Tyr_{\alpha 160}$: O^{η}	$Glu_{\alpha 165}$: $O^{\varepsilon 1,2}$	99.2
Arg_{C70}: $N^{\eta 1}$	$Tyr_{\alpha 160}$: O^{η}	56.3
$Asp_{\alpha 161}$: N	$Arg_{\alpha 166}$: O	86.9
$Asp_{\alpha 161}$: $O^{\delta 1}$	$Arg_{\alpha 122}$: $N^{\eta 2}$	76.3
$Asp_{\alpha 161}$: $O^{\delta 2}$	$Arg_{\gamma 122}$: $N^{\eta 1,2}$	98.4
$Ser_{\alpha 162}$: N	$Asp_{\alpha 161}$: $O^{\delta 1,2}$	84.4
$Lys_{\alpha 129}$: N^{ζ}	$Ser_{\alpha 162}$: O	78.0
$Thr_{\alpha 163}$: O^{γ}	$Gln_{\gamma 125}$: $O^{\varepsilon 1}$	65.3
$Ser_{\alpha 127}$: O^{γ}	$Thr_{\alpha 163}$: O	93.7
$Cys_{\alpha 164}$: N	$Thr_{\alpha 163}$: O^{γ}	51.7
$Arg_{\alpha 166}$: N	$Cys_{\alpha 164}$: O	60.1
$Tyr_{\alpha 168}$: N	$Arg_{\alpha 159}$: O	75.3

Percentage of the S1 MD trajectory is given with the corresponding hydrogen bond occurrence.

heterodimer complex. Distance between C^{α} atoms of C8γ Cys40 and C8α Cys164 residues respectively was found to fluctuate around 0.642 (0.020) nm. The corresponding distance between C8γ Ala_{40} and C8α Ala_{164} C^{α} atoms was found 0.637 and 0.590 nm in the non-covalent and covalent X-ray complexes respectively. Side chain dihedral angle χ^1 averaged at 174.9 (8.9°) and 176.4° (9.0°) in C8γ Cys_{40} and C8α Cys_{164} residues respectively. The corresponding values in the C8γ/C8α complex were found -74.1° and -62.1° respectively. This discrepancy in χ^1 dihedral angles can explain the small difference in C^{α} distance.

C8γ/C8α peptide interactions

The majority of protein/peptide interactions observed in the starting X-Ray structure [6] were also observed in the current MD study. For example side chain interaction between C8γ Arg_{122} and C8α indel peptide Asp_{161} was fully retained (Table 2). Hydrogen bond was also observed (93.7% of the simulation time) between C8γ Ser_{127}:O^{γ} and C8α indel peptide Thr_{163}:O. The distance in the crystal structure was found to be 0.345 nm. Another important interchain hydrogen bond that was observed was between C8γ Lys_{129}:N^{ζ} and C8α indel peptide Ser_{162}:O (78% of the simulation time). The corresponding distance in the crystal structure was 0.286 nm.

Trajectory of the non-covalent complex (S2)

As it can be seen from Fig. 3, both C8 α and γ chains of the non-covalent complex (S2) showed similar RMSF values of C^{α} atoms with the covalent complex (S1). Most RMSF values were found below 0.1 nm suggesting limited flexibility in complex's fluctuations. This fact indicates that the imposition of the disulfide bond had minor affection of the overall structure of the complex and did it alter its main structural features. Time series of RMSD backbone atoms are also shown in Fig. 3c. The indel peptide showed minimal fluctuation with RMSD values between 0.028 and

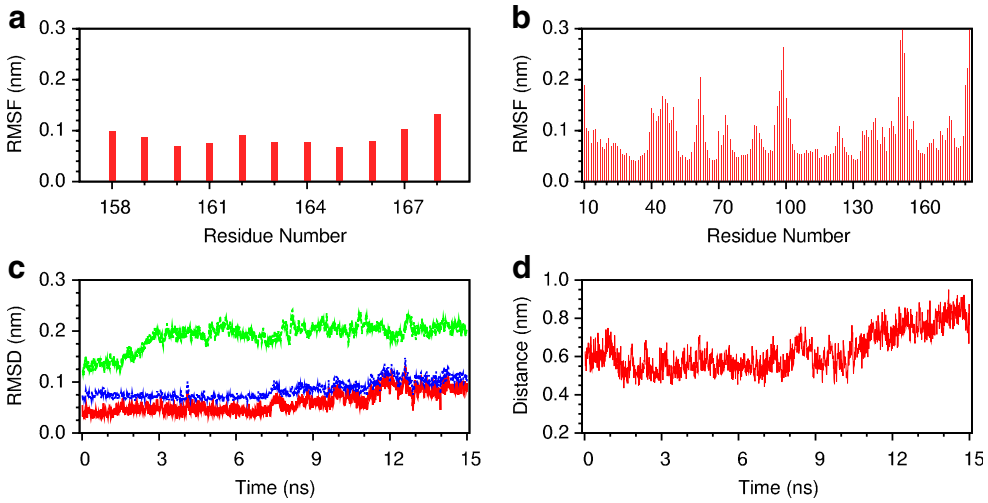

Fig. 3 Results from S2 (non-covalent structure) simulation. **a**) Root mean square fluctuation of the C^{α} atoms of the C8α indel peptide. **b**) Root mean square fluctuation of C^{α} atoms of the C8γ protein. **c**) Time evolution of RMSD of backbone atoms of C8α indel peptide over starting structure (red line), C8γ protein over starting structure (green line) and C8α indel peptide over the corresponding fragment of C8α protein complexed with C8γ (blue line). **d**) Time evolution between the distance of the side chain atoms C8γ Ala_{40}:C^{β} and C8α Ala_{164}:C^{β}. For the interpretation of colors in this figure the reader is referred to the online version of this article

0.132 nm which averaged at 0.060 nm (0.020 nm). Comparison of the trajectory frames of the indel peptide with the X-ray structure of the covalent complex (Fig. 3c) revealed very good structural similarity, with average RMSD value found at 0.085 nm (0.017 nm).

The distance between C8γ Ala_{40}:C^{α} and C8α Ala_{164}:C^{α} atoms is shown in Fig. 3d. These two residues were found in close contact in the X-ray structure and because of this it was supposed that they might serve as a connecting link through disulfide bond between the C8γ chain and the indel peptide (α chain). The distance fluctuated in the range (0.435 nm, 0.950 nm) and averaged at 0.623 nm (0.103 nm) in very good agreement with the corresponding distance found in X-Ray structure of the covalent complex (0.590 nm).

The secondary structure of the peptide was found in CCEETTTTEEC state for 93.2% of the time. Thus, its conformation was found more compact than in S1 (covalent complex). Bridge type conformational states (according to STRIDE assignment) found for residues Tyr_{160} or Leu_{167} in S1 (covalent complex) were only rarely observed in S2 (non-covalent complex). Main chain hydrogen bonds Arg_{159}←Tyr_{168} and Arg_{166}←Asp_{161} stabilizing the β-strand structure which were found in 91.3% and 52.1% of the simulation time respectively (Table 2).

As in the S1 case, two consecutive β-turns were observed in the middle part of the peptide sequence, instead of a $_{3\text{-}10}$helix found in residues Ser_{162}-Ala_{164} in the crystal structure. Residues Ser_{162}-Thr_{163} constituted the central part of the first turn, which was found to be type IV according to STRIDE analysis. Main chain hydrogen bond Asp_{161}←Cys_{164} that could stabilize this turn was not observed. Anyway, distance of C^{α} atoms of residues Asp_{161} and Cys_{164} and dihedral angle (absolute value) of C^{α} atoms of residues Asp_{161}-Ser_{162}-Thr_{163}-Cys_{164} remained below 0.7 nm and 90° respectively for 93.0% of the simulating time. The corresponding percentage of the second β-turn (fragment Ser_{162}-Thr_{163}-Cys_{164}-Glu_{165}) was found 100%.

Table 3 lists the hydrogen interactions found during S2 trajectory. In most cases, good agreement exist with the S1 trajectory, thus the same interactions were observed. Anyway, there are also differences observed mainly in the C-terminal part of the peptide. For example, intramolecular hydrogen bond interaction between backbone amide group of Cys_{164} and side chain hydroxyl group of Thr_{163} found in S1, was not observed during S2. Side chain of Asp_{161} replaced Thr_{163} in hydrogen bonding with backbone amide of Cys_{164} in 70.8% of the trajectory frames.

Table 3 Hydrogen bonding of the indel peptide (intramolecular hydrogen bonds) or the C8γ/peptide (intermolecular hydrogen bonds)

Donor	Acceptor	% in S2
$Arg_{\alpha 159}$: N	$Tyr_{\alpha 168}$: O	31.8
$Arg_{\alpha 159}$: $N^{\eta 2}$	$Tyr_{\alpha 168}$: O	58.5
$Tyr_{\alpha 160}$: O^{η}	$Glu_{\alpha 165}$: $O^{\varepsilon 1,2}$	98.1
Arg_{C70}: $N^{\eta 1}$	$Tyr_{\alpha 160}$: O^{η}	88.1
$Asp_{\alpha 161}$: N	$Arg_{\alpha 166}$: O	97.1
$Asp_{\alpha 161}$: $O^{\delta 1}$	$Arg_{\gamma 122}$: $N^{\eta 2}$	57.0
$Asp_{\alpha 161}$: $O^{\delta 2}$	$Arg_{\gamma 122}$: $N^{\eta 1,2}$	84.3
$Lys_{\gamma 129}$: N^{ζ}	$Ser_{\alpha 162}$: O	97.8
$Thr_{\alpha 163}$: O^{γ}	$Gln_{\gamma 125}$: $O^{\varepsilon 1}$	21.0
$Ser_{\gamma 127}$: O^{γ}	$Thr_{\alpha 163}$: O	92.7
$Cys_{\alpha 164}$: N	$Asp_{\alpha 161}$: $O^{\delta 1,2}$	70.8
$Arg_{\alpha 166}$: N	$Asp_{\alpha 161}$: O	52.1
$Tyr_{\alpha 168}$: N	$Arg_{\alpha 159}$: O	91.3

Percentage of the S2 MD trajectory is given with the corresponding hydrogen bond occurrence.

Concluding remarks

C8γ binds an indel peptide of C8α sequence and forms a non-covalent complex. A hypothesis has been made, based on crystallographic data, that the arrangement of this 11mer peptide corresponding to C8α complement protein into the binding calyx of C8γ could facilitate the disulfide linking between the two chains, thus a model of C8α/γ association can be drawn. Few facts about the 3D structure of MAC are yet known and this hypothesis, backed by crystallographic data, provided a very reasonable framework of C8α-γ association.

The results presented in this work corroborate the idea of this type of heterodimer formation by applying computational modeling and molecular dynamics simulations. Initially, substitution of C8α Ala164 and C8γ Ala40 of the crystal structure with cysteine residues and thus restoring the original sequence of the two protein chains, and subsequently modeling the disulfide bond linkage resulted in a reasonable heterodimer model of C8α-γ association. The structural stability of the complex was tested by applying molecular dynamics simulations. Computational modeling revealed minor fluctuations of the trajectory frames from the original crystal structure. The imposed disulfide linkage did not alter significantly the overall structure of the complex. The indel peptide of C8α complement protein retained its secondary structure, with only minor conformational transitions, within the C8γ binding calyx. Non-bonded interactions between the two chains were found to be stable during the MD trajectory and further stabilized the heterodimer complex. These findings suggest the tenability of the initial hypothesis about the C8α-γ type of association and provide further evidence for the nature of the covalently linked heterodimer.

Very recently Slade et al. [11] published the X-Ray structure of C8γ/C8α complex. The structural similarity of the indel peptide modeled in complexed form with disulfide bond with C8γ protein in the current study and the

corresponding fragment of the C8α protein (RMSD 0.08-0.14 nm, disulfide dihedral difference less than 10°) confirmed the validity of the proposed model.

Acknowledgment NAMD parallel execution was performed at the Research Center of Scientific Simulations (RCSS) of University of Ioannina. The open source community is gratefully acknowledged for making publicly available all the computational tools (Linux, NAMD, GNU tools, etc) needed for this research.

References

1. Muller-Eberhard HJ (1988) Molecular organization and function of the complement system. Annu Rev Biochem 57:321–347. doi:10.1146/annurev.bi.57.070188.001541
2. Steckel EW, York RG, Monahan JB, Sodetz JM (1980) The eighth component of human complement. Purification and physicochemical characterization of its unusual subunit structure. J Biol Chem 255:11997–12005
3. Ng SC, Gururaj Rao A, Zack Howard OM, Sodetz JM (1987) The eighth component of human complement: Evidence that it is an oligomeric serum protein assembled from products of three different genes. Biochemistry 26:5229–5233. doi:10.1021/bi00391a003
4. Ortlund E, Parker CL, Schreck SF, Ginell S, Minor W, Sodetz JM et al. (2002) Crystal structure of human complement protein C8gamma at 1.2 A resolution reveals a lipocalin fold and a distinct ligand binding site. Biochemistry 41:7030–7037. doi:10.1021/bi025696i
5. Hadders MA, Beringer DX, Gros P (2007) Structure of C8alpha-MACPF reveals mechanism of membrane attack in complement immune defense. Science 317:1552–1554. doi:10.1126/science.1147103
6. Lovelace LL, Chiswell B, Slade DJ, Sodetz JM, Lebioda L (2008) Crystal structure of complement protein C8gamma in complex with a peptide containing the C8gamma binding site on C8alpha: implications for C8gamma ligand binding. Mol Immunol 45:750–756. doi:10.1016/j.molimm.2007.06.359
7. Plumb ME, Sodetz JM (2000) An indel within the C8 alpha subunit of human complement C8 mediates intracellular binding of C8 gamma and formation of C8 alpha-gamma. Biochemistry 39:13078–13083. doi:10.1021/bi001451z
8. Slade DJ, Chiswell B, Sodetz JM (2006) Functional studies of the MACPF domain of human complement protein C8alpha reveal sites for simultaneous binding of C8beta, C8gamma, and C9. Biochemistry 45:5290–5296. doi:10.1021/bi0601860
9. Karplus M, McCammon JA (2002) Molecular Dynamics simulations of biomolecules. Nat Struct Biol 9:646–652. doi:10.1038/nsb0902-646
10. van Gunsteren WF, Dolenc J, Mark AE (2008) Molecular simulation as an aid to experimentalists. Curr Opin Struct Biol 18:149–153
11. Slade DJ, Lovelace LL, Chruszcz M, Minor W, Lebioda L, Sodetz JM (2008) Crystal structure of the MACPF domain of human complement protein C8alpha in Complex with the C8gamma Subunit. J Mol Biol 379:331–342. doi:10.1016/j.jmb.2008.03.061
12. Berman HM, Westbrook J, Feng Z, Gilliland G, Bhat TN, Weissig H et al. (2000) The Protein Data Bank. Nucleic Acids Res 28:235–242. doi:10.1093/nar/28.1.235
13. Humphrey W, Dalke A, Schulten K (1996) VMD: visual molecular dynamics. J Mol Graph 14:33–38. doi:10.1016/0263-7855(96)00018-5
14. Word JM, Lovell SC, Richardson JS, Richardson DC (1999) Asparagine and glutamine: using hydrogen atom contacts in the choice of side-chain amide orientation. J Mol Biol 285:1735–1747. doi:10.1006/jmbi.1998.2401
15. MacKerell AD et al (1998) All-atom empirical potential for molecular modeling and dynamics studies of proteins. J Phys Chem B 102:3586–3616. doi:10.1021/jp973084f
16. Jorgensen WL, Chandrasekhar J, Madura JD, Impey RW, Klein ML (1983) Comparison of simple potential functions for simulating liquid water. J Chem Phys 79:926–935. doi:10.1063/1.445869
17. Phillips JC et al (2005) Scalable molecular dynamics with NAMD. J Comput Chem 26:1781–1802. doi:10.1002/jcc.20289
18. Darden T, York D, Pedersen L (1993) Particle mesh Ewald: an N·log(N) method for Ewald sums in large systems. J Chem Phys 98:10089–10092. doi:10.1063/1.464397
19. Ryckaert JP, Ciccotti G, Berendsen HJC (1977) Numerical integration of the Cartesian equations of motion of a system with constraints: molecular dynamics of n-alkanes. J Comput Phys 23:327–341. doi:10.1016/0021-9991(77)90098-5
20. Feller SE, Zhang YH, Pastor RW, Brooks BR (1995) Constant pressure molecular dymanics simulation: The Langevin Piston method. J Chem Phys 103:4613–4621. doi:10.1063/1.470648
21. Glykos NM (2006) Carma: a molecular dynamics analysis program. J Comput Chem 27:1765–1768. doi:10.1002/jcc.20482
22. Frishman D, Argos P (1995) Knowledge-based protein secondary structure assignment. Proteins 23:566–579. doi:10.1002/prot.340230412
23. Delano W (2002). The PYMOL Molecular Graphics System (Delano Scientific, San Carlos, CA)